

Comparison of DDBD with FBD procedures for concentrically braced steel frame



J. Goggins & S. Salawdeh

National University of Ireland, Galway

SUMMARY:

A Direct Displacement Based Design (DDBD) methodology is compared to a Forced Based Design (FBD) methodology for concentrically braced frames (CBFs). The comparison is carried out by designing 4 and 12-storey CBF buildings using both DDBD and FBD methodologies. The performance for both methodologies is verified using nonlinear time history analysis (NLTHA) employing eight different accelerograms with displacement response spectra matching the design displacement spectrum. It is found that the seismic base shear, F_b , from the FBD is larger than the base shear obtained from DDBD. This leads to the use of larger sections for the structure designed by the FBD approach to resist the lateral forces. Because of that, the lateral displacements the structure endures in the FBD approach are less than the design lateral displacements used to design the structure in DDBD approach.

Keywords: Concentrically braced frames, Force based design, Direct displacement based design.

1. INTRODUCTION

A comparison between two common design philosophies that exist in seismic design of structures will be presented in this paper. They are force based design (FBD) and direct displacement based design (DDBD). Current design procedures such as EC8 (CEN 2004) use FBD. Calvi and Sullivan (2009) published codified provisions for DDBD and work is on-going for extending the DDBD methodology.

1.1. Force based design (FBD) procedure

In FBD, preliminary estimates of member sizes should be carried out at the start of the design in order to estimate the elastic stiffness needed to find the fundamental period using either Equation 1.1 or eigenvalue analysis. Seismic codes use empirical expressions for the period based on a general description of the structural system and its geometry. EC8 (CEN 2004) approximates the period, T in seconds, for buildings with heights of up to 40 m by the following expression:

$$T = C_t H^{3/4} \quad (1.1)$$

where C_t is 0.085 for moment resistant space steel frames, 0.075 for moment resistant space concrete frames and for eccentrically braced steel frames, and 0.05 for all other structures, H is the height of the building, in metres, from the foundation or from the top of a rigid basement.

To take into account the capacity of the structure to dissipate energy, FBD uses the design spectrum, S_d . This can be obtained by reducing the ordinates of the reference elastic spectrum, S_e , by means of a behaviour factor, q , which allows for the ductility expected for the structural system. Seismic codes specify values for the behaviour factor, q , depending upon the material of construction and the type of structural system used. However, these values appear to be arbitrary and difficult to justify. By finding

the design spectrum, S_d , the design base shear can be found and distributed to the floors. Then the structure can be analysed under the lateral distributed seismic forces and the structural design of members that are selected to dissipate energy can be carried out and the displacements under the seismic actions can be estimated.

If the calculated displacements exceed the code limits, redesign is required. If the calculated displacements are satisfactory, the members that are not expected to dissipate energy by remaining elastic can be designed using the capacity design methodology.

Priestley (1993; 2003) critically examined the force based seismic design procedure. He suggested that the current emphasis on strength-based seismic design, based on elastic structural characteristics, modified by behaviour factors leads designers in directions that are not always rational. Some of the shortcomings associated with FBD outlined by Priestley et al. (2007) are summarised as follows:

- FBD relies on estimates of initial stiffness to determine the period and the distribution of design forces between different structural elements. Since the stiffness is dependent on the strength of the elements, this cannot be ascertained until the design process is complete.
- Allocating seismic force among elements based on initial stiffness (even if accurately known) is illogical for many structures, because it incorrectly assumes that the different elements can be forced to yield simultaneously.
- FBD is based on the assumption that unique force reduction factors (based mainly on system ductility demand) are appropriate for a given structural type and material. However, ductility demand for individual structural members significantly differs from the system ductility depending upon geometry of the structure, flexibility of the capacity protected elements and foundation flexibility.

1.2. Direct displacement based design (DDBD)

As a result of the shortcoming of the force based design approach identified by Priestley (1993; 2003), Priestley et al. (2007) published a book on displacement based seismic design (DDBD) of structures in order to mitigate the deficiencies in current FBD. This has led to codified provisions for DDBD being published by Calvi and Sullivan (2009). The fundamental property of the DDBD is characterising the structure to be designed by a single degree of freedom (SDOF) model with a peak displacement response. This representation is based on the substitute structure approach carried out by Gulkan and Sozen (1974) and Shibata and Sozen (1976).

The DDBD method characterises the structure to be designed by a single degree of freedom (SDOF) representation of performance at peak displacement response. While force-based seismic design characterises the structure in terms of elastic, pre-yield, properties (initial stiffness, K_i , elastic damping, ξ_n), DDBD characterises the structure by the secant stiffness, K_e , at maximum displacement Δ_D .

For a given level of ductility demand, DDBD characterises the structure with a level of equivalent viscous damping, ξ_{eq} , representative of the combined elastic damping and the hysteretic energy absorbed during inelastic response. After determining the design displacement at maximum response, Δ_D , and the corresponding damping estimated from the expected ductility demand, ξ_{eq} , the effective period, T_e , at maximum displacement response, measured at the effective height, H_e , can be read from a set of displacement spectra for different levels of damping. Then the effective stiffness, K_e , of the equivalent SDOF system at maximum displacement, Δ_D , can be found and the design based shear, F_b , can be estimated. A flow chart of the DDBD procedure for CBFs is shown in Figure 1.1.

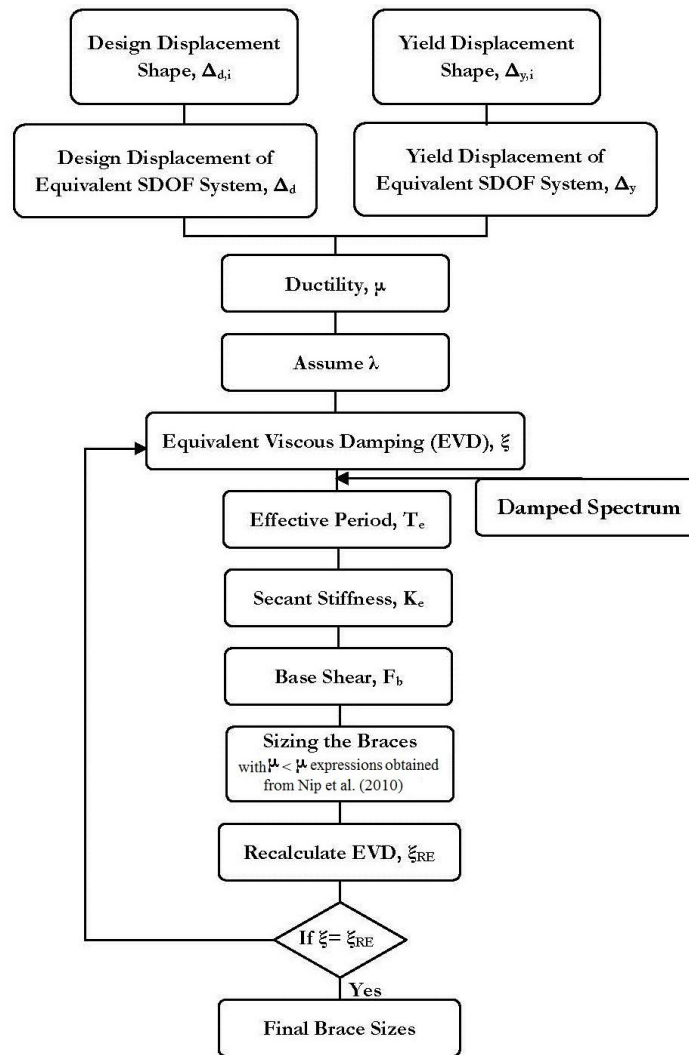


Figure 1.1. Flow chart of the DDBD procedure for CBFs adapted from (Wijesundara 2009).

2. CASE STUDIES FOR CBFs TO BE USED FOR DDBD AND FBD METHODOLOGIES.

Two case studies of 4- and 12-storey buildings are designed to compare the DDBD and FBD methodologies for steel CBFs. The building's dimensions are 32m by 32m in plan consisting of two CBFs in each direction as the lateral resisting frames, as shown in Figure 2.1. These buildings are symmetric in plan and elevation with a uniform storey height of 3m. For simplicity, stiffness and strength contributions of the interior partitions and the exterior cladding are ignored and the accidental torsion is neglected. Plan view and elevation for the 4-storey structure are shown in Figure 2.1. Columns are assumed to be continuous along the height and pinned at the base. The connections between columns and beams are assumed to be pinned and the lateral forces are assumed to be resisted by the braces on the 4m bays represented by the dashed line. Bracing end conditions are considered to be pinned in both ends. Characteristic dead and imposed loads of 8.1KPa and 3KPa, respectively, were selected using provisions of EC1 (CEN 2004). Seismic loads were taken as the summation of the unfactored dead load and a reduced live load (seismic load = $G_k + 0.3 \cdot Q_k = 8.1 + 0.3 \cdot 3 = 9$ KPa, where G_k is the characteristic dead load and Q_k is the characteristic imposed load). Grade S355 steel with nominal yield strength of 355N/mm^2 was chosen for all elements. Eurocode 8 (CEN 2004) type 1 elastic response spectrum for soil type C and peak ground acceleration (PGA) of 0.3g was chosen. Design storey drifts of 2.5% were selected to control damage of non-structural elements. Section sizes and slenderness ratios of the braces for the 4-storey and 12-storey CBF case studies found using DDBD and FBD are shown in Table 2.1 and 2.2, respectively.

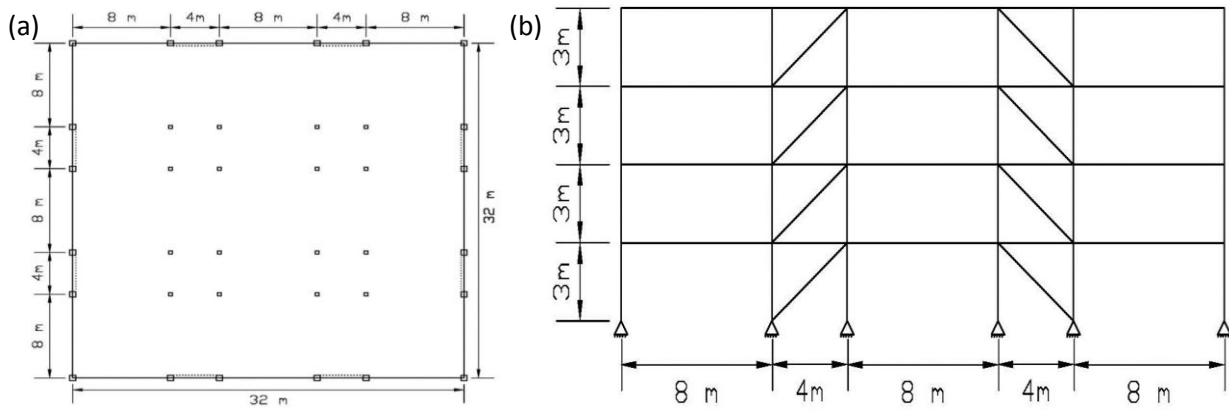


Figure 2.1. (a) Plan view of the four storey CBF case study. (b) Elevation of the 4-storey CBF case study.

Table 2.1. Section sizes and slenderness ratios for the 4-storey CBF case study using DDBD and FBD.

Level	DDBD		FBD	
	section size	$\bar{\lambda}$	section size	$\bar{\lambda}$
4	100X100X10	1.80	140X140X10	1.26
3	150X150X10	1.15	200X200X12	0.87
2	150X150X12.5	1.17	250X250X12	0.69
1	160X160X12.5	1.09	300X300X12	0.56

Table 2.2. Section sizes and slenderness ratios for the 12-storey CBF case study using DDBD and FBD.

Level	DDBD		FBD	
	section size	$\bar{\lambda}$	section size	$\bar{\lambda}$
12	120X120X6.3	1.42	200X200X8	0.84
11	120X120X10	1.47	260X260X10	0.64
10	120X120X12.5	1.51	260X260X12.5	0.65
9	140X140X12.5	1.27	300X300X16	0.57
8	160X160X12.5	1.09	450X250X16	0.64
7	180X180X12.5	0.96	400X400X16	0.42
6	180X180X14.2	0.97	400X400X16	0.42
5	180X180X16	0.99	400X400X20	0.43
4	180X180X16	0.99	400X400X20	0.43
3	200X200X16	0.88	400X400X20	0.43
2	200X200X16	0.88	400X400X20	0.43
1	200X200X16	0.88	400X400X20	0.43

3. VERIFICATION OF DDBD AND FBD PROCEDURES

In order to verify the performance of the design methodologies used to design the CBF case studies, non-linear time history analyses (NLTHA) are carried out with time histories having displacement spectra that match the design displacement spectrum used in the DDBD application. The computer programme used for the verification is OPENSEES (McKenna et al. 2000).

3.1 Numerical model

Two-dimensional numerical models are employed, in which columns and beams are modelled to behave elastically. The connections between columns and beams, as well as between beams and braces, are assigned as pinned connections. Columns are assumed to be continuous along the height and pinned at the base. Braces are modelled as nonlinear beam-column element with distributed plasticity, where the cross section of the brace is divided into fibres along the perimeter and across the thickness. In this model, the brace is divided into a minimum of two elements using ten integration points per element. An initial camber of 1% of the length of the brace is applied to the middle of the

brace to account for the overall buckling. This camber is applied in in-plane direction to have in-plane buckling. A low cyclic fatigue model is used to wrap the fibre based nonlinear beam column model in order to capture fracture in the braces. Uniaxial Giuffre-Menegotto-Pinto steel material model with isotropic strain hardening and monotonic envelop is used in this study with a value of strain hardening equal to 0.008.

The numerical integration method used to evaluate the dynamic response of the structure is Hilber-Hughes-Taylor (HHT) method, which is an extension to the Newmark method with constant Gamma equal to 0.5. Rayleigh damping model is used which assumes that the damping matrix is proportional to the mass and stiffness matrices. Elastic damping of 3% was specified. Similar value was found from physical tests (Broderick et al. 2008) and used in DDBD methodology. The numerical model was verified using cyclic tests of brace members and real-time full-scale shake table tests for single storey CBF structures (Salawdeh and Goggins 2011a; Salawdeh and Goggins 2011b).

3.2. Ground motions used in the study

Eight accelerograms from four different earthquakes (2 components in orthogonal direction for each earthquake) taken from Pennucci et al. (2009) are used in the NLTHA, as shown in Table 3.1.

Table 1.1. Properties of the first set ground motions.

Earthquake	ID used	Date	PEER ID	Magnitude, M	Distance, r (km)
Northridge	EQ3a, EQ3b	Jan. 17, 1994	959	6.7	5
Imperial Valley	EQ4a, EQ4b	Oct. 15, 1979	169	6.5	34
Hector	EQ5a, EQ5b	Oct. 16, 1999	1762	7.13	48
Landers	EQ6a, EQ6b	Jun. 28, 1992	900	7.28	86

Time history accelerograms are scaled to get a displacement response spectrum that matches the soil type C design displacement spectrum with 5% damping from EC8 (CEN 2004), which was used in the DDBD for the case studies. Response spectra for the scaled accelerograms are found using the programme SeismoSignal (SeismoSoft 2007) for the elastic response spectra with 5% damping, as shown in Figure 3.1.

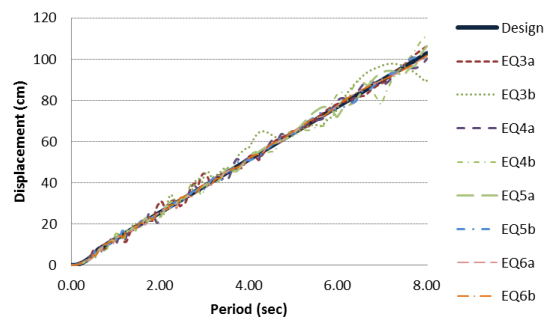


Figure 3.1. 5% design spectrum compared to the scaled displacement spectra for eight accelerograms used to verify the design procedure using NLTHA.

3.3. Comparison of results from NLTHA and DDBD

For the 4-storey and the 12-storey CBF structures, the maximum floor displacements, taking into account the higher modes effect, are found during NLTHA for the eight accelerograms. These are compared with the design displacement profile obtained from the DDBD method, as shown in Figure 3.2. Similarly, the average of the maximum recorded displacement during time-history analyses for the eight accelerograms and the design displacement profile employed in the DDBD are shown in Figure 3.3 for the 4-storey and the 12-storey buildings. It is apparent that the maximum displacements recorded from the time history analyses for the 4-storey and the 12-storey buildings are conservatively representing the linear design displacements assumed. One possible reason is that in the design it was

assumed that the tension brace only resists the earthquakes, as per the provisions of Eurocode 8 (CEN 2004). However, it is found that the compression brace also contributes to the lateral resistance in CBFs (Goggins 2004). Furthermore, 10% of the base shear was assigned to be resisted by top floor to account for the higher mode effects, which leads to stronger upper storeys.

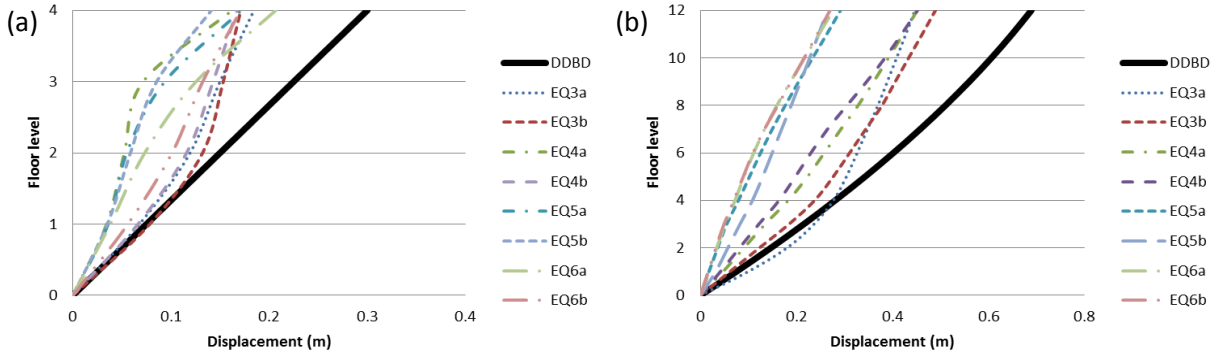


Figure 3.2. (a) Maximum recorded displacements for eight spectrum compatible accelerograms compared with the design displacements employed in the DDBD methodology for (a) 4-storey and (b) 12-storey CBFs.

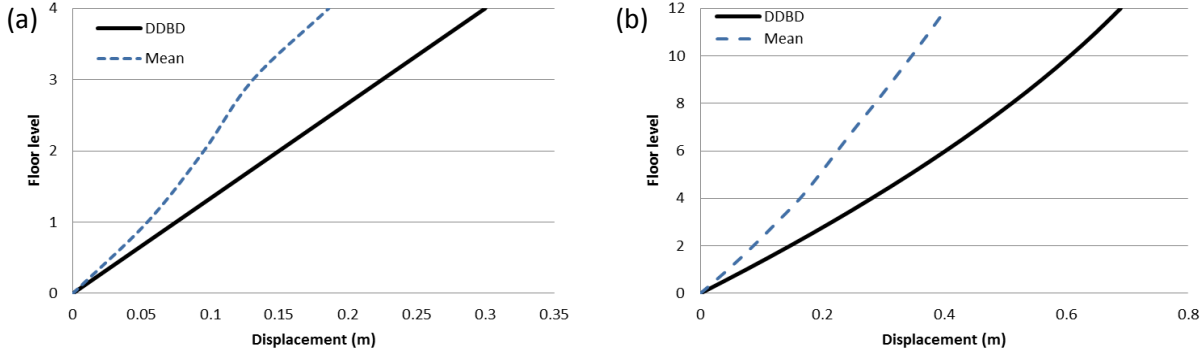


Figure 3.3. Average of the maximum recorded displacements for eight spectrum compatible accelerograms compared with the design displacements employed in the DDBD for the (a) 4-storey and (b) 12-storey CBFs.

The average of the maximum storey drifts recorded during time-history analyses using the eight accelerograms compared with the linear displacement design drift profile assumed for the case studies are shown in Figure 3.4 for the 4-storey and 12-storey buildings. It is found that the average of the maximum recorded storey drifts for the eight accelerograms for the 4-storey and 12-storey buildings are conservatively less than the design storey drift profile for the reasons mentioned earlier.

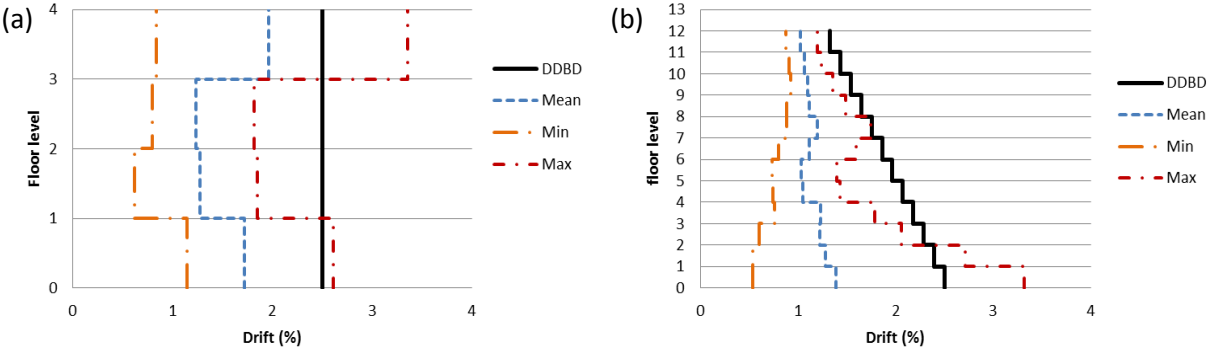


Figure 3.4. Average of the maximum recorded storey drifts for eight spectrum compatible accelerograms compared with the design storey drifts employed in the DDBD for the (a) 4-storey and (b) 12-storey CBF.

The maximum recorded ductility values are found during NLTHA for the eight accelerograms for the 4-storey and the 12-storey buildings and are compared with the design ductility values obtained from the DDBD method in Figure 3.5. It is evident that the maximum ductility observed in the time history analyses for the 4-storey and the 12-storey CBFs are in general less than the ductility used in the design. The main reason for this is that in the design, the lateral forces in the structure induced by the earthquakes were assumed to be resisted by the tension brace members only. However, the base shear is resisted by braces in both tension and compression, albeit the contribution of the compression member is significantly less than that of the tension member.

The average of the maximum recorded ductility during time-history analyses for the eight accelerograms is shown in Figure 3.6 for the 4-storey and the 12-storey buildings. This is compared to the design ductility obtained from the DDBD method, ductility expressions established by Nip et al. (2010) for hot-rolled and cold-formed steel, which are given in Equations (3.1) and (3.2), respectively, and ductility expression established by Tremblay (2002) shown in Equation (3.3). It is apparent that the average of the maximum ductility values recorded from the time history analyses for the 4-storey and the 12-storey buildings are lower than the design ductility from the DDBD method, as well as ductility expressions established by Nip et al. (2010) and Tremblay (2002).

$$\mu_f = 3.69 + 6.97\bar{\lambda} - 0.05(b/t\varepsilon) - 0.19(\bar{\lambda})(b/t\varepsilon) \tag{3.1}$$

$$\mu_f = 6.45 + 2.28\bar{\lambda} - 0.11(b/t\varepsilon) - 0.06(\bar{\lambda})(b/t\varepsilon) \tag{3.2}$$

$$\mu_f = 2.4 + 8.3\bar{\lambda} \tag{3.3}$$

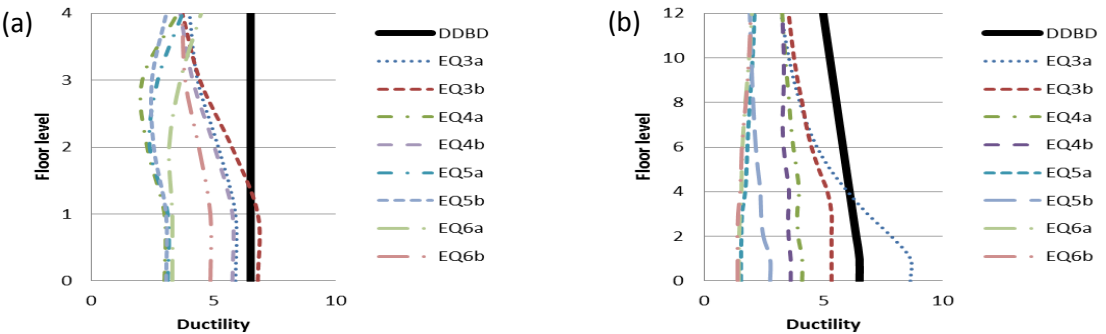


Figure 3.5. Maximum recorded ductility for eight spectrum compatible accelerograms compared with the design ductility assumed in the DDBD for (a) 4-storey CBF and (b) 12-storey CBF.

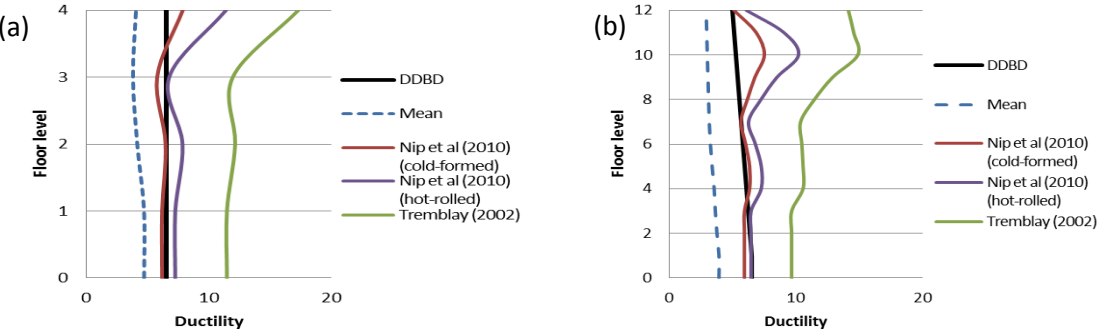


Figure 3.6. Average of the maximum recorded ductility for eight spectrum compatible accelerograms compared to the design ductility and other ductility expressions for (a) 4-storey CBF and (b) 12-storey CBF.

4. COMPARISON OF FBD APPROACH WITH DDBD AND NLTHA

In this section a comparison is carried out between the 4- and 12-storey structures designed using the DDBD approach with those designed using the FBD approach. Furthermore, the predicted performance of the structure designed using the FBD approach is obtained using NLTHA and salient response parameters are discussed.

When comparing the 4- and 12-storey case studies designed using both the DDBD and FBD approaches, it is found that the seismic base shear, F_b , from the FBD is larger than the base shear obtained from DDBD. This leads to the use of larger sections for the structure designed by FBD approach to resist the lateral forces. Because of that, the lateral displacements the structure endures in the FBD approach are less than the design lateral displacements used to design the structure in DDBD approach. Furthermore, the larger base shear forces experienced in the structure designed using the FBD approach will lead to higher demands on foundations.

The maximum floor displacements are found during NLTHA for the eight accelerograms for the 4- and 12-storey case studies that were designed according to the FBD approach. These are compared with the displacement profile obtained from FBD approach as per the Eurocode 8 provisions (CEN 2004) and the design displacement profile used in DDBD, as shown in Figure 4.1. Similarly, the average of the maximum recorded displacement during NLTHA for the eight accelerograms is compared with the displacement profile obtained from FBD and the design displacement profile employed in DDBD in Figure 4.2. It is apparent that the maximum displacements recorded from the NLTHA and from the FBD approach are less than the linear design displacements assumed for the DDBD procedure.

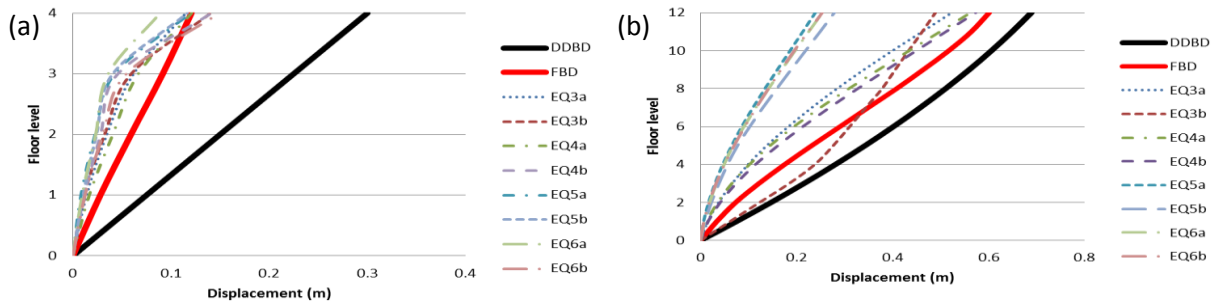


Figure 4.1. Maximum recorded displacements in the NLTHA compared with the design displacements used for the DDBD and the displacements obtained from FBD approach for (a) 4-storey (b) 12-storey CBFs.

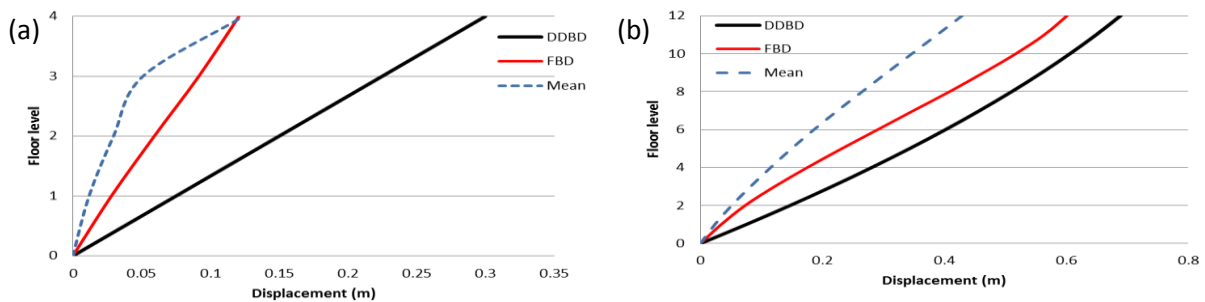


Figure 4.2. Average of the maximum recorded displacements in the NLTHA compared with the design displacements used for the DDBD and the displacements obtained from FBD approach for (a) 4-storey (b) 12-storey CBFs.

The average of the maximum recorded storey drifts for the eight accelerograms for the 4-storey and 12-storey buildings are less than the design storey drift profile obtained from FBD and used in DDBD for most of the storeys (Figure 4.3). This is due to the design assumption that the tension brace member only is assumed to contribute to the lateral resistance of the system. On the other hand, the

average maximum drift obtained from the NLTHA was more than the design drift for the top storey due to higher mode effects. Because of that and in order to take into account the higher modes effect, 10% of the base shear force should be allocated for to the roof level and the remaining 90% of the base shear force should be distributed to all floor levels including the roof in proportion to the product of mass and displacement, as suggested by Priestley et al. (2007). This is the approach taken in the DDBD method used above.

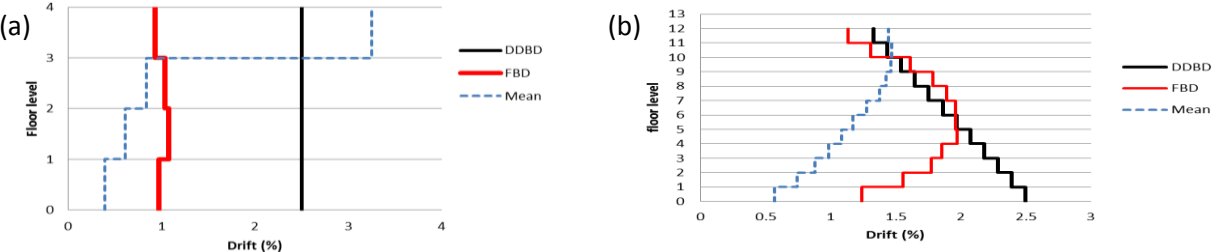


Figure 4.3. Average of the maximum recorded storey drifts for eight spectrum compatible accelerograms compared with the design storey drifts used for the DDBD and the drifts obtained from FBD approach for the (a) 4-storey (b) 12-storey CBFs.

The maximum recorded ductility values found during NLTHA of the case study buildings that were designed using the FBD methodology and subjected to eight accelerograms are compared with the design ductility values obtained from the FBD and DDBD methods in Figure 4.4. It is found that the maximum ductility demands estimated from NLTHA for the case studies are in general very close to the ductility found from the FBD approach and less than the ductility used in the DDBD. This is due to the larger section sizes required in the structure designed using the FBD approach.

The average of the maximum recorded ductilities during time-history analyses for the eight artificially adjusted accelerograms are shown in Figure 4.5 for the case study buildings. These are compared to the design ductilities obtained from the FBD and the DDBD methods, as well as ductility expressions established given in Equations (3.1) to (3.3). It is apparent that the average of the maximum ductility values recorded from NLTHA for the case study buildings designed according to FBD provisions are close to the design ductility obtained from FBD and lower than the design ductility from the DDBD method and ductility expressions established by Nip et al. (2010) and Tremblay (2002).

CONCLUSIONS

Two case studies of 4- and 12-storey CBF buildings are designed using DDBD and FBD approaches, and then the performance is gauged with NLTH analyses. The comparison showed that FBD approach

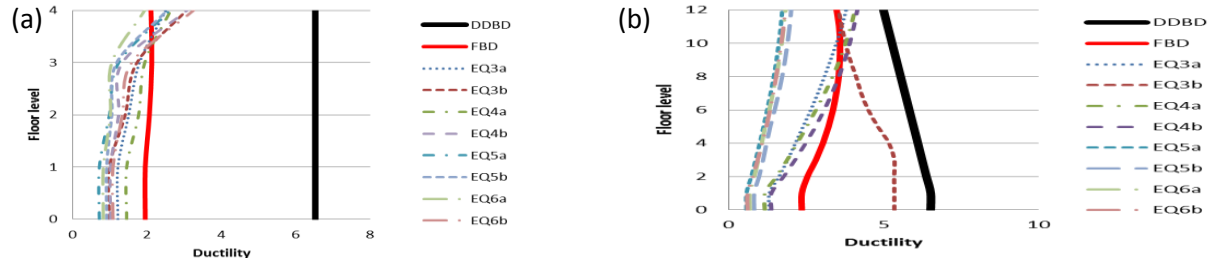


Figure 4.4. Maximum recorded ductility for eight spectrum compatible accelerograms compared with the design ductility from DDBD and FBD method for the (a) 4-storey and (b) 12-storey CBFs.

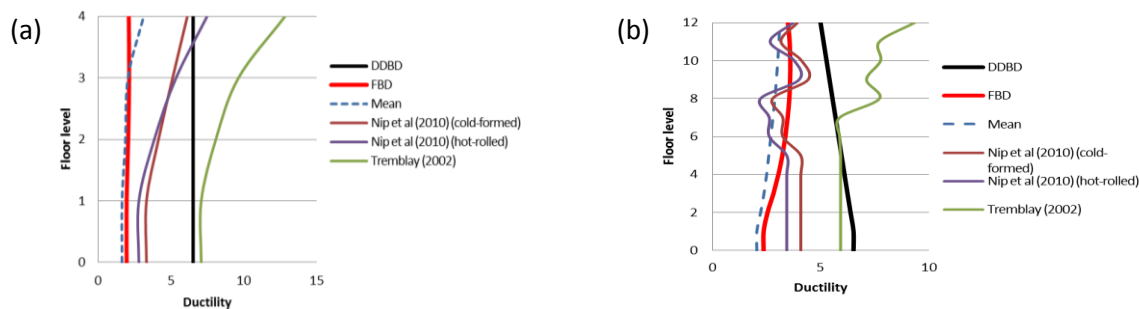


Figure 4.5. Average of the maximum recorded ductility for eight accelerograms compared to the design ductility from DDBD and FBD approach and other ductility expressions for the (a) 4-storey and (b) 12-storey CBFs.

gives larger section sizes for the same earthquake demand on the building. This leads to lower displacement shapes and storey drifts than the DDBD approach.

Moreover, the NLTHA indicated that FBD is conservative for displacement shapes and storey drifts for all storeys except the top floor, which leads to the need of taking into account the higher mode effects on FBD.

ACKNOWLEDGEMENT

The second author acknowledges the financial support provided by NUIG through the CoEI Fellowship.

REFERENCES

- Broderick, B. M., A. Y. Elghazouli and J. Goggins (2008). "Earthquake testing and response analysis of concentrically-braced sub-frames." *Journal of Constructional Steel Research* **64**: 997-1007.
- Calvi, G. M. and T. J. Sullivan (2009). Development of a Model Code for Direct Displacement Based Seismic Design. G. Manfredi, M. Dolce (eds), *The state of Earthquake Engineering Research in Italy: the ReLUIS-DPC 2005-2008 Project*. Napoli, Italy.
- CEN (2004). Eurocode 1.General actions. Part 1-1: Densities, self-weight, imposed loads for buildings. EN 1991-1-1.
- CEN (2004). Eurocode 8, design of structures for earthquake resistance – Part 1: General rules, seismic actions and rules for buildings, EN 1998-1:2004/AC:2009.
- Goggins, J. (2004). *Earthquake resistant hollow and filled steel braces*. Doctoral dissertation, Ph.D. thesis, Trinity College, University of Dublin.
- Nip, K. H., L. Gardner and A. Y. Elghazouli (2010). "Cyclic testing and numerical modelling of carbon steel and stainless steel tubular bracing members." *Engineering Structures* **32**(2): 424-441.
- Priestley, M. J. N. (1993). "Myths and fallacies in earthquake engineering.-conflicts between design and reality." *Bulletin of the NZ National Society for Earthquake Engineering* **26**(3) 329-334.
- Priestley, M. J. N. (2003). Myths and fallacies in earthquake engineering, revisited. Mallet Milne lecture. IUSS Press. Pavia, Italy.
- Priestley, M. J. N., G. M. Calvi and M. J. Kowalsky (2007). *Displacement-Based Seismic Design of Structures*, IUSS Press, Pavia, Italy.
- Salawdeh, S. and J. Goggins (2011a). Validation of a numerical model for use in non-linear time history analysis of CBFs *The Eighth International Conference on Structural Dynamics EUROSDYN2011*. Leuven, Belgium.
- Salawdeh, S. and J. Goggins (2011b). Numerical model for the seismic response of cold formed steel braces. *The 6th International Conference on Thin Walled Structures*. Timisoara, Romania.
- Tremblay, R. (2002). "Inelastic seismic response of steel bracing members." *Journal of Constructional Steel Research* **58**(5-8): 665-701.
- Wijesundara, K. K. (2009). *Design of concentrically braced steel frames with RHS shape braces*. Doctoral dissertation, Ph.D. thesis, European Centre for Training and Research in Earthquake Engineering (EUCENTRE).